ORIGINAL ARTICLE

Susanna Herold · Franz-Josef K. Rehmann

Kinetic and mechanistic studies of the reactions of nitrogen monoxide and nitrite with ferryl myoglobin

Abstract Nitrogen monoxide (nitric oxide) generated endogenously has a variety of different properties. Among others it regulates blood pressure and transmission of nerve impulses, and has been shown to exert specific toxic effects, but also, paradoxically, to protect against various toxic substances. Recent studies suggest that NO· can serve as an antioxidant of the highly oxidizing ferryl myoglobin (MbFe^{IV}=O), which has been proposed to be at least in part responsible for the oxidative damage caused by the reperfusion of ischemic tissues. In the present work we have determined the rate constant for the reaction between MbFe^{IV}=O and NO· [$(17.9\pm0.5)\times10^6$ M^{-1} s^{-1} at pH 7.5 and 20 °C] and we have shown that this reaction proceeds via the intermediate nitrito-metmyoglobin complex MbFe^{III}ONO. Our results imply that this reaction is very likely to take place in vivo and might indeed represent a detoxifying pathway for both MbFe^{IV}=O as well as NO·. Moreover, we have found that the rate of reaction of MbFe^{IV}=O with nitrite is significantly lower (16 ± 1 M^{-1} s^{-1} at pH 7.5 and 20 °C). Thus, this reaction probably plays a role only when NO· has been consumed completely and large concentrations of nitrite are still present. In contrast to the protecting role of NO·, the reaction with nitrite generates nitrogen dioxide which can contribute to tyrosine nitration. Indeed, we have demonstrated that nitrite can nitrate added tyrosine in the presence of iron(III) myoglobin and hydrogen peroxide.

Keywords Nitrogen monoxide · Nitrite · Ferryl myoglobin · Nitrotyrosine · Kinetics

S. Herold (✉) · F.-J.K. Rehmann
Laboratory of Inorganic Chemistry, ETH Zürich,
Universitätsstrasse 6, 8092 Zürich, Switzerland
E-mail: herold@inorg.chem.ethz.ch
Phone: +41-1-6322858
Fax: +41-1-6321090

Abbreviations *Compound I*: (porphyrin·$^+$) oxoiron(IV) · *Compound II*: (porphyrin)oxoiron(IV) · *Hb*: hemoglobin · *HbFeO$_2$*: oxyhemoglobin · *metHb*: iron(III) hemoglobin · *His*: histidine · *HRP*: horseradish peroxidase · *LPO*: lactoperoxidase · *Mb*: myoglobin · *MbFe^{II}*: deoxymyoglobin · *MbFeO$_2$*: oxymyoglobin · *metMb*: iron(III) myoglobin · *MbFe^{IV}=O*: ferryl [oxoiron(IV)] myoglobin · *·MbFe^{IV}=O*: ferryl myoglobin with a transient protein radical · *MPO*: myeloperoxidase · *NO$_2$-Tyr*: 3-nitrotyrosine · *Tyr*: tyrosine · *Tyr·*: tyrosyl radical

Introduction

The mechanism of tissue damage caused by reperfusion of an ischemic tissue is not well understood yet. It has been proposed to be triggered by the formation of reactive oxygen and nitrogen species such as superoxide, hydrogen peroxide, hydroxyl radical, and peroxynitrite [1, 2, 3, 4]. The reaction between hydrogen peroxide (present in concentrations as high as 10 μM in ischemic heart muscle [5]) and myoglobin has been suggested to be a key determinant of oxidative damage in the ischemic and then reoxygenated heart [6]. Hydrogen peroxide reacts with deoxymyoglobin, MbFe^{II} (also present in elevated concentration in ischemic oxygen-poor tissues), to generate the highly oxidizing species ferryl myoglobin, MbFe^{IV}=O. In addition, the reaction of metmyoglobin with hydrogen peroxide generates the one-electron oxidized form of MbFe^{IV}=O, which has an additional transient radical on the globin, ·MbFe^{IV}=O [7]. The radical species generated from this reaction can damage the cell membrane, induce the release of myoglobin from ruptured myocytes, and thus lead to destabilization and subsequent liberation of free iron, providing the potential for hydroxyl radical formation [2, 8]. There is direct evidence that the high oxidation state of myoglobin

($Fe^{IV}=O$) is formed in vivo. Indeed, it has been identified, through derivatization with Na_2S to form sulfomyoglobin, [9] in isolated ischemic rat hearts [10].

$MbFe^{IV}=O$ is a strong oxidant that can promote oxidation, peroxidation [8, 11, 12], and epoxidation of various biomolecules in vitro [7]. The reaction of several antioxidant species such as β-carotene, ascorbate, thiols, and vitamin E with ferryl myoglobin has been the subject of various studies [7]. The reduction rates are mostly not very large [13]. For instance, the rate constant for the reaction of $MbFe^{IV}=O$ with ascorbate (present in micromolar concentrations in several cells) is 2.7 ± 0.8 M^{-1} s^{-1} at pH 7.0 and 25 °C [13]. However, it has been proposed that the presence of these one-electron reductants may be essential to avoid the accumulation of $MbFe^{IV}=O$ and thus to prevent cell damage in reperfused tissues.

It has repeatedly been reported that also $NO^.$ (nitrogen monoxide, nitric oxide) may act as an antioxidant and inhibit $MbFe^{IV}=O$-induced oxidative damage [3, 14, 15, 16, 17, 18, 19]. Indeed, $NO^.$ can reduce $MbFe^{IV}=O$ to metMb [14, 16], modulate $MbFe^{IV}=O$-mediated oxidation of low-density lipoproteins [14], and inhibit $^.MbFe^{IV}=O$-catalyzed oxidation reactions [16]. Despite the physiological importance attributed to the reaction between $NO^.$ and $MbFe^{IV}=O$, its rate constant has never been determined. This information is indispensable in order to evaluate the relevance of this reaction in vivo.

As nitrite is one of the major end products of $NO^.$ metabolism, its local concentration reflects that of $NO^.$. Increased nitrite levels are thus found under pathophysiological conditions such as inflammation, when $NO^.$ production is elevated. For instance, high levels of nitrite have been found in synovial fluids of patients with rheumatoid arthritis [20] and nitrite concentrations as high as 36 µM have been measured in human serum of immunodeficiency virus-infected patients with interstitial pneumonia [21].

In contrast to the protective properties of $NO^.$ against H_2O_2-mediated tissue injuries, nitrite dramatically enhances H_2O_2 toxicity, in particular in the presence of hemoproteins [22]. It has been suggested that the increased toxicity is due to the formation of nitrogen dioxide from the reaction of nitrite with the ferryl form of proteins such as myoglobin and peroxidases. Nitrogen dioxide is a toxic substance known to react with thiols [23], to cause lipid peroxidation [17, 24], and to damage DNA [17, 22]. Moreover, the peroxidase-catalyzed oxidation of nitrite has been proposed to represent an alternative source of tyrosine nitration [25]. In addition to the peroxynitrite-mediated nitration [26, 27, 28], it may contribute to cell and tissue injury under conditions of increased $NO^.$ production. The biological significance of tyrosine nitration is a subject of great interest, because extensive evidence supports the formation of nitrotyrosine in vivo in diverse pathological conditions (for review see [28]).

In this paper we present detailed kinetic and mechanistic studies on the reactions of $MbFe^{IV}=O$ with $NO^.$ and with nitrite. The rate constant determined for the $NO^.$-mediated reduction of $MbFe^{IV}=O$ is very large, $(17.9\pm0.5)\times10^6$ M^{-1} s^{-1} at pH 7.5 and 20 °C. Thus, we conclude that this reaction is very likely to represent a plausible route for inhibition of $MbFe^{IV}=O$-mediated oxidative damage. In contrast, the reaction between nitrite and $MbFe^{IV}=O$ is relatively slow, 16 ± 1 M^{-1} s^{-1} at pH 7.5 and 20 °C. This reaction probably plays a role only when $NO^.$ has been completely depleted and no peroxynitrite is present. The results reported are important for a better understanding of the interaction of $NO^.$ with hemoproteins with oxidase activity under inflammatory or ischemic conditions, when generation of both $NO^.$ and H_2O_2 is elevated.

Materials and methods

Reagents

Buffer solutions were prepared from K_2HPO_4/KH_2PO_4 (Fluka) or from $Na_2B_4O_7.10H_2O/NaOH$ (Fluka) with deionized Milli-Q water. Sodium nitrite, sodium nitrate, and hydrogen peroxide were supplied from Fluka. Catalase (bovine liver, 17,000 units/mg protein) was obtained from Sigma.

Nitrogen monoxide was obtained from Linde and passed through a degassed NaOH solution as well as a column of NaOH pellets to remove higher nitrogen oxides before use. A saturated $NO^.$ solution was prepared by degassing water for 45 min with N_2 and then saturating it with $NO^.$. The obtained stock solution (ca. 2 mM) was diluted with degassed buffer in gas-tight SampleLock Hamilton syringes. The final $NO^.$ concentrations were measured with an ANTEK Instruments nitrogen monoxide analyzer, with a chemiluminescent detector.

Horse heart metmyoglobin was purchased from Sigma and purified over a Sephadex G-25 column. The concentration of H_2O_2 was determined spectrophotometrically at 240 nm ($\varepsilon_{240}=39.4$ M^{-1} cm^{-1}) [29]. $MbFe^{IV}=O$ was prepared by adding 7–15 equiv of H_2O_2 to a metMb solution at room temperature. After a reaction time of 5–20 min, depending on the pH, the $MbFe^{IV}=O$ solutions were stored on ice and used within 1 h. In some cases, catalase was added prior to reaction with $NO^.$ to destroy excess H_2O_2. However, this procedure proved not to be necessary as identical kinetic results were obtained with or without addition of catalase. The concentration of the metMb solutions was determined by measuring the absorbances at 408, 502, and 630 nm ($\varepsilon_{408}=188$ mM^{-1} cm^{-1}, $\varepsilon_{502}=10.2$ mM^{-1} cm^{-1}, and $\varepsilon_{630}=3.9$ mM^{-1} cm^{-1}) at neutral pH as well as at acidic pH, and at 411, 539, and 585 nm ($\varepsilon_{411}=119$ mM^{-1} cm^{-1}, $\varepsilon_{539}=8.8$ mM^{-1} cm^{-1}, and $\varepsilon_{585}=7.8$ mM^{-1} cm^{-1}) at pH 9.5 [30]. The concentrations of the $MbFe^{IV}=O$ solutions were determined by measuring the absorbance at 421 nm ($\varepsilon_{421}=111$ mM^{-1} cm^{-1}) [31].

Stopped-flow kinetic analysis

Kinetic studies were carried out with an On-Line Instrument System stopped flow instrument equipped with an OLIS RSM 1000 rapid scanning monochromator and with an Applied Photophysics SX17MV single-wavelength stopped-flow instrument. The pathlengths of the cells in the two spectrophotometers were 2 and 1 cm, respectively. With the Applied Photophysics apparatus, kinetic traces were taken at different wavelengths between 400 and 635 nm and the data were analyzed with the SX17MV

operating software or with Kaleidagraph, version 3.0.5. Traces (averages of at least 10 single traces) from at least five experiments were averaged to obtain each observed rate constant, given with the corresponding standard error. Care was taken that the absolute absorbance of the reaction mixture was not higher than one absorbance unit.

For the measurements between pH 6.5 and 9.5 the MbFe^{IV}=O and NO$^\cdot$ solutions were both prepared in 0.1 M buffers of the required pH value. Measurements at pH 5.9 were carried out by mixing a MbFe^{IV}=O solution prepared in a 0.1 M phosphate buffer at pH 6.5 with a NO$^\cdot$ solution at pH 4.0. The pH was measured at the end of the reactions for control.

UV-visible spectra

UV-visible spectra were collected on a UVIKON 820 spectrophotometer. To determine the yield of the reaction between NO$^\cdot$ and MbFe^{IV}=O, spectra were measured in sealable cells for anaerobic applications. About 3 mL of a 100 µM metMb solution were placed in the cell and mixed with ca. 3 equiv of H_2O_2 (100 µL of a 0.01 M solution). When the MbFe^{IV}=O had completely formed the cell was sealed and about 150 µL of NO$^\cdot$-saturated solution were added.

Ion chromatographic product analysis

Product analysis was carried out by anion chromatography with conductivity detection with a Metrohm Instrument (ICSeparation Center 733, ICDetector 732, and IC pump 709) equipped with an Anion SUPER-SEP (6.1009.000) column and an Anion SUPER-SEP (6.1009.010) precolumn as described previously [32]. A phthalic acid solution (2.5 mM phthalic acid, 5% acetonitrile, pH 4.2, Tris) was used as eluent. Calibration curves were obtained by measuring 5–10 standard sodium nitrite and sodium nitrate solutions in 1 mM sodium phosphate buffer.

The protein samples were prepared by adding 7–15 equiv H_2O_2 to 20 mL of a metMb solution (25–50 µM in 2 mM phosphate or 1 mM borate buffer). After a reaction time of 5–20 min, that is when the UV-visible spectrum indicated that MbFe^{IV}=O had been formed completely, excess H_2O_2 was destroyed by addition of about 100 µL of a solution of catalase in water (1 mg/mL). After 10 min the solution was placed in a 20 mL Schlenk flask, sealed with a rubber septum, and the required amount of NO$^\cdot$ (250–500 µL of a saturated 2 mM NO$^\cdot$ solution) was added with a gas-tight Hamilton syringe under constant stirring. A long needle was used in order to add the NO$^\cdot$ solution at the bottom of the flask to avoid any contact of NO$^\cdot$ with the oxygen present in the head space of the flask. After about 5 min the reaction mixture was diluted with buffer and analyzed. The amount of contaminating nitrite and nitrate present in the NO$^\cdot$ solution was determined prior to each experiment by injecting 1 mL of the saturated NO$^\cdot$ solution with a gas-tight syringe into 9 mL of O_2-saturated water placed in a sealed 10 mL Schlenk flask. After stirring for about 10 min the reaction mixture was diluted and analyzed. With this procedure, nitrite is quantitatively formed from the reaction of NO$^\cdot$ with O_2 in water. Thus, the amount of nitrite found in excess relative to the NO$^\cdot$ used for these experiments corresponded to the amount of nitrite already present in the NO$^\cdot$ solution. In some cases also nitrate was found as a contaminant and probably derived from oxygen impurities in the apparatus. The protein samples of the reactions with nitrite were prepared analogously by adding 100–200 µL of a 40–60 mM sodium nitrite solution in 0.1 M phosphate buffer.

Analysis of the free nitrotyrosine content generated by the reaction of nitrite with ferryl myoglobin in the presence of added free tyrosine

MbFe^{IV}=O, prepared by mixing 1.5 mL of a 295 µM metMb solution with one equivalent of H_2O_2 (44 µL of a 0.01 M solution), was allowed to react with a solution containing 4 equiv of tyrosine and different amounts of nitrite (between 4 and 50 equiv). The final solution, which contained 250 µM protein, was analyzed by HPLC (see Table 6 below, entries 1–3) with a Hewlett Packard Series 1050 apparatus with a Series 1100 UV/Vis-Detector, equipped with a VYDAC 218TP54 Protein&Peptide C18-Column (250×4.6 mm). Solvent A was 0.07% TFA in H_2O and solvent B was 0.07% TFA in acetonitrile. Nitrotyrosine (NO$_2$-Tyr) was eluted (ca. 8 min after injection) by keeping the amount of B constant (5%) in the first 2 min and then by using an increasing linear gradient of B from 5 to 10% between 2 and 10 min, and from 10 to 80% between 10 and 15 min. NO$_2$-Tyr was detected contemporaneously at 220, 280, 350, and 400 nm and was quantified by measuring a calibration curve of 5–10 NO$_2$-Tyr standard solutions.

Alternatively, reactions were carried out by mixing 1.5 mL of a 295 µM metMb solution containing 4 equiv of tyrosine and different amounts of nitrite (between 4 and 50 equiv) with a solution containing 1 equiv of H_2O_2 (relative to the protein). The resulting protein solution, which contained 250 µM protein, was analyzed by HPLC as described above (see Table 6 below, entries 4–7).

Analysis of the nitrotyrosine content after reaction of ferryl myoglobin with NO$^\cdot$ and nitrite

A $^\cdot$MbFe^{IV}=O solution in 0.1 M phosphate buffer, pH 7.0, was prepared by adding 1 equiv of H_2O_2 to metMb (320 µM) [33, 34]. After 80 s, the time needed for generation of $^\cdot$MbFe^{IV}=O, different amounts of NO$^\cdot$ (0.1 or 0.5 equiv) were added under stirring. When the reaction was complete (in less than 1 min), nitrite was removed by washing the solution through a 10,000 MW cut-off filter (Centriplus YM-10, Amicon, Switzerland) at 3000g until the ultrafiltrate did not show any qualitative reaction (pink coloring) with the Griess reagent [35]. The resulting protein was hydrolyzed by treating it (0.5 mL of a 320 µM solution) for 24 h with 0.3 mL 6 M HCl at 100 °C in a closed vial. The solution was allowed to dry in air by maintaining the temperature at 100 °C and by opening the vial. The residual was redissolved in 50 µL H_2O and analyzed by HPLC as described above.

The NO$_2$-Tyr content in myoglobin after reaction of MbFe^{IV}=O with nitrite was measured analogously. A MbFe^{IV}=O solution in 0.1 M phosphate buffer, pH 7.0, prepared by adding 2 equiv of H_2O_2 to a metMb solution (160 µM), was allowed to react with nitrite (either 0.2 or 10 equiv). When the reaction was over (in less than 1 min), nitrite was washed by centrifugation (see above), the resulting protein was hydrolyzed, and the amino acids were analyzed by HPLC as described above.

Results

Stopped-flow kinetic studies of the NO$^\cdot$-mediated reduction of ferryl myoglobin

The reaction between NO$^\cdot$ and MbFe^{IV}=O (horse heart) was studied by single-wavelength stopped-flow spectroscopy in the pH range 5.9–9.5 at 20 °C. In order to avoid the difficulties associated with the accurate determination of the concentration of NO$^\cdot$ solutions during the measurements, the protein was present in
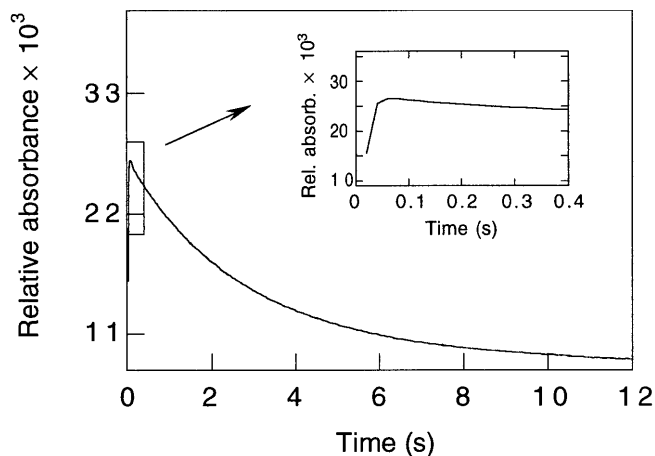
Fig. 1 Time course measured at 411 nm for the reaction of $MbFe^{IV}=O$ (8.1 μM) with $NO^.$ (0.9 μM) in 0.1 M borate buffer at pH 9.5 and 20 °C
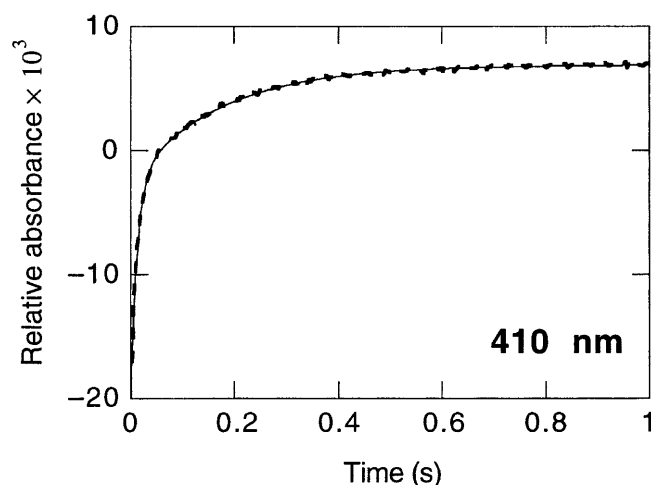

Fig. 2 Time course measured at 410 nm for the reaction of $MbFe^{IV}=O$ (4.7 μM) with $NO^.$ (0.6 μM) in 0.1 M phosphate buffer at pH 7.0 and 20 °C. The *solid line* corresponds to the best fit for the formation and the decay of the intermediate $MbFe^{III}ONO$. The resulting rate constants are $k_{1,obs}=80\pm1$ s^{-1} and $k_{2,obs}=5.80\pm0.05$ s^{-1}, respectively

8- to 10-fold excess to maintain pseudo-first-order conditions. The kinetic traces were measured by following the absorbance changes at several wavelengths in the Soret region. Over the entire pH range studied the reaction proceeds via an intermediate that decays to the final product metMb. As depicted in Fig. 1, the kinetic trace collected at pH 9.5 at 411 nm clearly shows a rapid increase in the absorbance followed by a slower decrease. At pH 7.0 the trace measured at 410 nm shows a biphasic increase in absorbance which could be fitted well to two single-exponential expressions (Fig. 2). In both cases the two reactions correspond to the formation of the intermediate and its subsequent decay. The second-order rate constants (k_1) for the formation of the intermediate, obtained
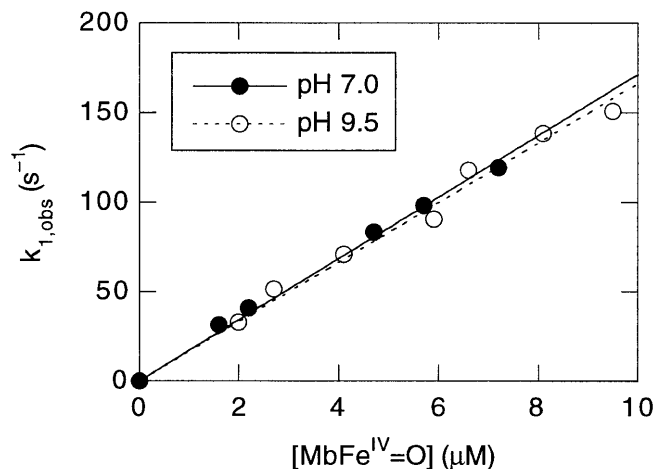

Fig. 3 Plots of $k_{1,obs}$ versus $MbFe^{IV}=O$ concentration for the formation of the intermediate $MbFe^{III}ONO$ from the reaction of $MbFe^{IV}=O$ with $NO^.$ at pH 7.0 and 9.5 (20 °C). The values of the second-order rate constants obtained from the linear fits are given in Table 1

from the linear plots of the observed pseudo-first-order rate constants versus $MbFe^{IV}=O$ concentration (Fig. 3), did not change significantly in the pH range studied (Fig. 3 and Table 1). At pH 7.5 we obtained $k_1=(17.9\pm0.5)\times10^6$ M^{-1} s^{-1} for the $NO^.$-mediated reduction of $MbFe^{IV}=O$. The same value for the second-order rate constant was obtained when the reaction was studied with $NO^.$ as the reagent used in 10-fold excess. Moreover, the same rate constant was also found when $MbFe^{IV}=O$ was prepared at pH 8.5 and then mixed with a pH 6.5 solution of $NO^.$ to yield a final pH of 7.0. Alkaline conditions are known to generate the lowest amount of side products in the course of the reaction between $MbFe^{IV}=O$ and H_2O_2 [36, 37].

As expected, the rate constant for the decay of the intermediate to metMb (k_2), measured within a broad range of $NO^.$ and $MbFe^{IV}=O$ concentrations, was independent from the $NO^.$ as well as the $MbFe^{IV}=O$ concentrations. Moreover, the same rate constant was obtained when either of the two reagents was used in excess. When $NO^.$ was used in large excess, an additional reaction was observed on a longer time scale which corresponded to $NO^.$ binding to the product metMb. The rate of decay of $MbFe^{III}ONO$ is highly

Table 1 pH dependencies of the second-order rate constants for the formation (k_1) of the intermediate $MbFe^{III}ONO$ and of the observed rate constants for its decay (k_2) to metMb at 20 °C

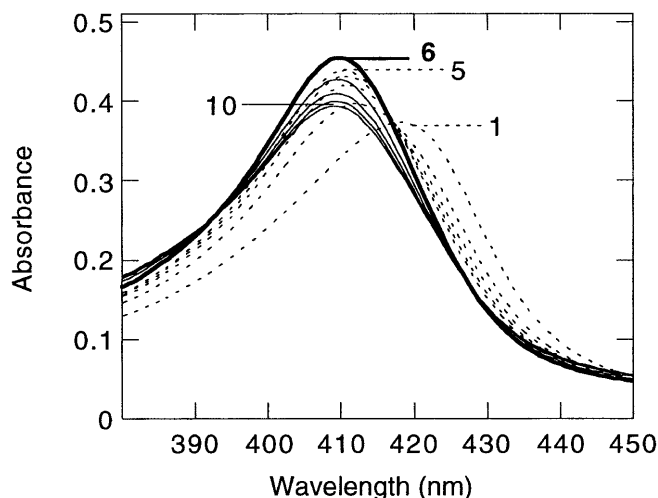| pH	k_1 (μM^{-1} s^{-1})	k_2 (s^{-1})
5.9	17.0±0.5	21.0±0.9
6.5	18.7±0.2	10.8±0.3
7.0	17.1±0.3	5.98±0.06
7.5	17.9±0.5	3.36±0.05
8.5	19.5±0.1	1.26±0.03
9.5	16.6±0.4	0.347±0.006

Fig. 4 Rapid-scan UV-visible spectra of the reaction of MbFe^{IV}=O (3.7 µM) with NO$^.$ (4.7 µM) in 0.1 M borate buffer at pH 9.5 and 20 °C. The formation of the intermediate MbFe^{III}ONO (*trace 6*) from MbFe^{IV}=O (*dashed traces 1–5*) and its decay to metMb (*traces 6–10*) are presented. Time intervals of the shown spectra are: traces 1–5, every 16 ms; trace 6, after 320 ms; traces 7–9, every 1.6 s; and trace 10, after a total of 9.84 s

Fig. 5 Rapid-scan UV-visible spectra of the reaction of MbFe^{IV}=O (14.7 µM) with NO$^.$ (50 µM) in 0.1 M borate buffer at pH 9.5 and 20 °C. The decay of the intermediate MbFe^{III}ONO to metMb is presented. Time intervals of the shown spectra are: traces 1–6, every 400 ms; trace 7, 8 s later; for a total of 10 s

pH dependent and increases with decreasing pH (Table 1). At pH 7.5 we obtained k_2=3.36±0.05 s^{-1} for the rate of decay of the intermediate to metMb.

Spectral characterization of the nitrito intermediate MbFe^{III}ONO

The NO$^.$-mediated reduction of MbFe^{IV}=O to metMb was studied by rapid-scan UV-visible spectroscopy between 380 and 680 nm at pH 9.5 and 20 °C. As shown in Fig. 4, the Soret band of myoglobin shifted from 421 nm (MbFe^{IV}=O, spectrum 1) to 411 nm (metMb at pH 9.5, spectrum 10) via an intermediate species with an absorption maximum at 410 nm and an extinction coefficient of about 137 mM^{-1} cm^{-1} (spectrum 6 in Fig. 4). The best spectrum obtained for the intermediate in the visible region is shown as the first trace in Fig. 5. As higher concentrations were used to reduce the signal-to-noise ratio, accumulation of the intermediate occurred within the dead time of the instrument. Two characteristic absorption maxima were found at 631 nm (ε_{631}=5.1 mM^{-1} cm^{-1}) and 504 nm (ε_{504}=8.7 mM^{-1} cm^{-1}). These maxima are very similar to those of the recently characterized peroxynitrito-methemoglobin complex (HbFe^{III}OONO) [38] and are typical for high-spin metHb and metMb derivatives with anionic oxygen ligands such as carboxylates [30], nitrite [39], and nitrate (Table 2). We thus assign this species as the nitrito-metmyoglobin complex MbFe^{III}ONO (Scheme 1).
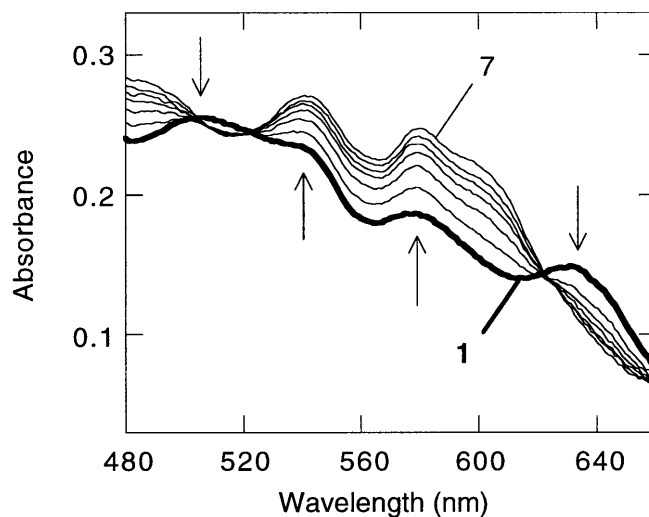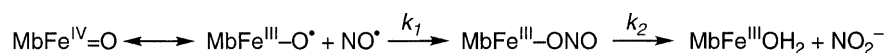
Table 2 Spectroscopic data for metmyoglobin complexes

	Soret	Visible		Ref
	λ_{max} $(\varepsilon)^a$	λ_{max} $(\varepsilon)^a$	λ_{max} $(\varepsilon)^a$	
MbFe^{III}ONO	410 (137)	504 (8.7)	534sh	This work
		575 (6.3)	631 (5.1)	
MbFe^{III}NO$_2$	412 (137)	502 (8.4)	537sh	[58]
		573 (5.4)	628 (4.2)	
MbFe^{III}ONO$_2$	404 (172)	502 (8.8)	629 (3.6)	[58]
MbFe^{III}OONO	410 (138)	504 (8)	636 (3.2)	[58]
MbFe^{III}OH$_2$	408 (188)	502 (10.2)	630 (3.9)	[30]

$^a\lambda_{max}$ in nm; ε in mM^{-1} cm^{-1}

UV-visible spectra of the protein product and yield of the reaction

In order to determine the stoichiometry of the reaction of NO$^.$ with MbFe^{IV}=O and the purity of the metMb formed, the reaction products were analyzed by UV-visible spectroscopy. As shown in Fig. 6, when about one equivalent of NO$^.$ was mixed with MbFe^{IV}=O at pH 7.0 a species was formed (spectrum C) with an absorbance spectrum similar but not identical to that of metMb (spectrum A). In particular, a new absorbance band with a maximum around 590 nm appeared and the band at 630 nm was modified as well. However, when a MbFe^{IV}=O solution was allowed to decay back to metMb, a very similar altered spectrum was obtained (spectrum D in Fig. 6) (as in [40]). The new absorbance band at 590 nm is
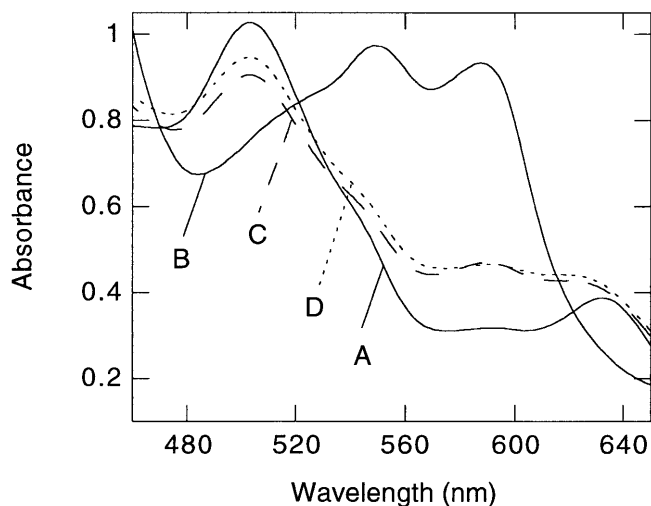
Scheme 1

$$MbFe^{IV}{=}O \longleftrightarrow MbFe^{III}{-}O^\bullet + NO^\bullet \xrightarrow{k_1} MbFe^{III}{-}ONO \xrightarrow{k_2} MbFe^{III}OH_2 + NO_2^-$$

Fig. 6 UV-visible spectra in 0.1 M phosphate buffer at pH 7.0. *A* $MbFe^{III}OH_2$ (100 μM); *B* $MbFe^{IV}=O$ (100 μM); *C* $MbFe^{IV}=O$ (100 μM) $NO^\cdot$ (110 μM); *D* $MbFe^{IV}=O$ (100 μM) decayed to $MbFe^{III}OH_2$ after ca. 2.5 h
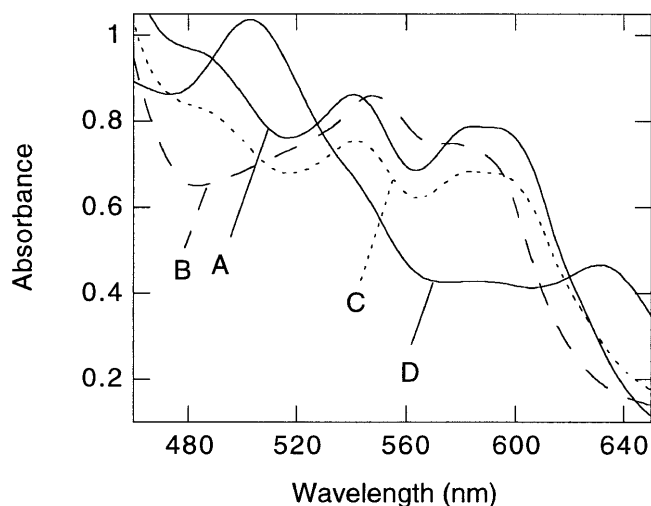
Fig. 7 UV-visible spectra in 0.1 M borate buffer at pH 9.5. *A* $MbFe^{III}OH$ (100 μM); *B* $MbFe^{IV}=O$ (100 μM); *C* $MbFe^{IV}=O$ (100 μM) $NO^\cdot$ (110 μM); *D* spectrum C at pH 7.0

characteristic for a heme-protein cross-linked form. This species is known to be partly generated in the course of the reaction of H_2O_2 with metMb under acidic as well as neutral conditions [41] and is thus already present in the $MbFe^{IV}=O$ solution.

It has previously been shown [36, 37] that the reaction between metMb and H_2O_2 proceeds with the minimum amount of side reactions between pH 8.0 and 9.0. $MbFe^{IV}=O$ was thus generated by mixing metMb and H_2O_2 at pH 8.5. When this solution was allowed to react with one equivalent of solution of $NO^\cdot$ at pH 6.5, the spectrum of the product obtained at a final pH of 7.0 was identical to that of metMb (data not shown). Furthermore, as shown in Fig. 7,

when about one equivalent of $NO^\cdot$ was mixed with $MbFe^{IV}=O$ at pH 9.5, a species was formed (spectrum C) with an absorbance spectrum almost identical to that of metMb under the same conditions (spectrum A). When this reaction solution was neutralized to pH 7.0 the new spectrum (spectrum D in Fig. 7) was identical to that of metMb at pH 7.0 (spectrum A in Fig. 6).

Reaction between $^\cdot MbFe^{IV}=O$ and $NO^\cdot$

It has been reported that in concentrated solutions (300 μM to 1 mM) metMb reacts with equimolar amounts of H_2O_2 to yield a two-electron oxidized form with a radical on the protein ($^\cdot MbFe^{IV}=O$) [33, 34]. The radical in $^\cdot MbFe^{IV}=O$ is probably localized on a tyrosine and/or a tryptophan residue and is stable for several minutes [33, 34]. An attempt was thus made, by using the sequential stopped-flow technique, to study the reaction between $^\cdot MbFe^{IV}=O$ and $NO^\cdot$. In particular, we were interested to find out whether $NO^\cdot$ reacts with the oxoiron(IV) center or with the radical on the protein.

A $^\cdot MbFe^{IV}=O$ solution was first generated in the stopped-flow apparatus by premixing equimolar amounts of metMb and H_2O_2 (ca. 350 μM). After a delay time between 10 and 500 s the $^\cdot MbFe^{IV}=O$ solution was mixed with a $NO^\cdot$ solution. The reaction was studied by following the absorbance changes at 540 and 590 nm. Unfortunately, we could not obtain any useful information from the first 50 ms of the measured traces because of inhomogeneous mixing. This problem is often observed when highly concentrated viscous protein solutions are mixed in the stopped-flow apparatus. Thus, it was not possible to identify whether there was a difference in the absorbance changes arising from the reaction of $NO^\cdot$ with $MbFe^{IV}=O$ and those from the reaction with $^\cdot MbFe^{IV}=O$.

It has recently been shown that the reaction of $NO^\cdot$ with the tyrosyl radicals of prostaglandin H synthase [42], prostaglandin endoperoxide H synthase [43], and photosystem II [44, 45] generates nitrotyrosine. Therefore, we looked for nitrotyrosine in the protein after the reaction of $^\cdot MbFe^{IV}=O$ with $NO^\cdot$. However, HPLC analysis of the amino acids obtained after complete acid hydrolysis indicated that no nitrotyrosine was generated (data not shown).

Stopped-flow kinetic studies of the nitrite-mediated reduction of ferryl myoglobin

The reaction between nitrite and $MbFe^{IV}=O$ was studied by rapid-scan stopped-flow spectroscopy between 380 and 650 nm. As shown in Fig. 8, when a large excess of nitrite was mixed with $MbFe^{IV}=O$ at pH 7.0 the Soret band shifted from 421 nm ($MbFe^{IV}=O$, spec-
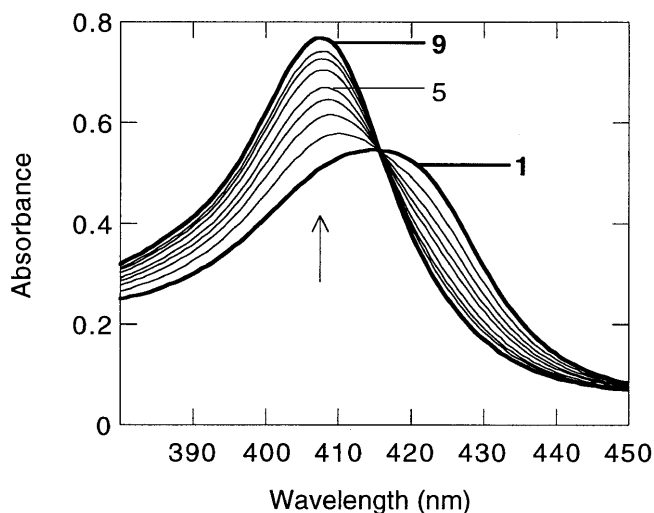
Fig. 8 Rapid-scan UV-visible spectra of the reaction of MbFe^{IV}=O (5.5 µM) with nitrite (9.6 mM) in 0.1 M phosphate buffer at pH 7.0 and 20 °C. Time intervals of the shown spectra are: traces 1–5, every 800 ms; traces 6–8, every 1.6 s; trace 9, after a total of 25.6 s

Fig. 10 Comparison of the UV-visible spectra of the intermediate MbFe^{III}ONO and of MbFe^{III}NO$_2$ in 0.1 M phosphate buffer at pH 7.0

Fig. 9 Rapid-scan UV-visible spectra of the reaction of MbFe^{IV}=O (78 µM) with nitrite (9.6 mM) in 0.1 M phosphate buffer at pH 7.0 and 20 °C. Time intervals of the shown spectra are: traces 1–5, every 800 ms; traces 6–8, every 1.6 s; trace 9, after a total of 25.6 s

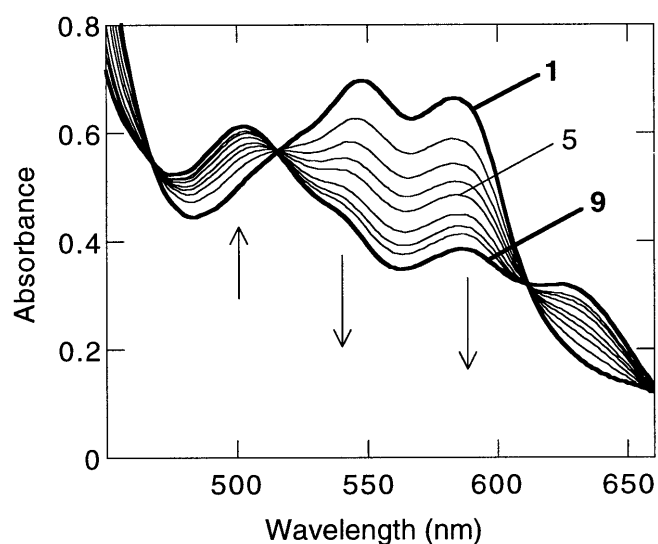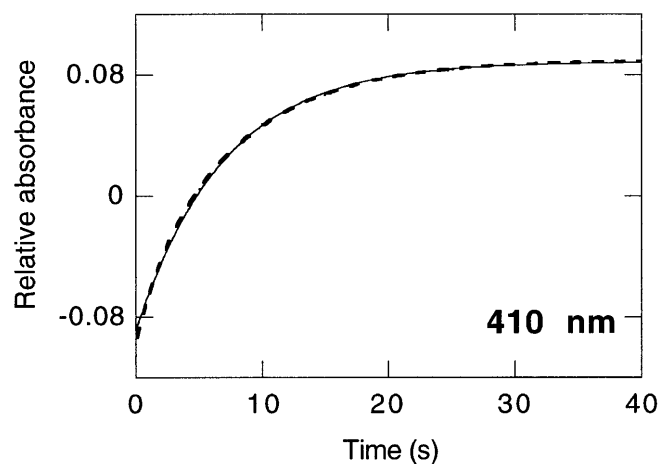**Fig. 11** Time course measured at 410 nm for the reaction of MbFe^{IV}=O (6 µM) with nitrite (2.0 mM) in 0.1 M phosphate buffer at pH 6.7 and 20 °C. The *solid line* corresponds to the best fit, which results in the observed rate constant of $(14.4\pm0.1)\times10^{-2}$ s^{-1}

trum 1) to 408 nm (metMb at pH 7.0, spectrum 9). In addition, the two characteristic absorption maxima at 547 and 584 nm disappeared and the characteristic maxima for metMb at 502 and 630 nm appeared (Fig. 9). However, an additional band was observed at 586 nm, that is at a slightly lower wavelength than that of the maximum arising from the cross-linked species generated during the synthesis of MbFe^{IV}=O (590 nm, see above). As MbFe^{III}NO$_2$ has an absorbance maximum at 573 nm (Fig. 10), the new absorb-

ance band at 586 nm suggests the formation of a mixture of metMb, the cross-linked species, and MbFe^{III}NO$_2$.

Kinetic measurements were carried out by single-wavelength stopped-flow spectroscopy under pseudo-first-order conditions with nitrite in at least 10-fold excess in the pH range 6.1–8.5 at 20 °C. The kinetic traces, measured by following the absorbance increases at 410 nm, could all be fitted well to a single-exponential expression (Fig. 11). The second-order rate constants (k_3), obtained from the linear plots of the observed pseudo-first-order rate constants versus nitrite concentration (data not shown), are highly pH dependent (Table 3). At pH 6.1 we obtained k_3=(3.7±

Table 3 pH dependencies of the second-order rate constants for the reactions of nitrite with MbFe^{IV}=O (k_3) at 20 °C. pH dependencies of the association (k_4) and dissociation (k_{-4}) rates of the reaction of nitrite with metMb at 20 °C together with the calculated equilibrium constants (K_4)

pH	k_3 (M^{-1} s^{-1})	k_4 (M^{-1} s^{-1})	k_{-4} (s^{-1})	K_4 (M)
6.1	$(3.7\pm0.4)\times10^2$	$(2.4\pm0.1)\times10^3$	19±2	$(0.80\pm0.08)\times10^{-2}$
6.7	65±3	$(8.1\pm0.2)\times10^2$	9.8±0.3	$(1.21\pm0.02)\times10^{-2}$
7.0[a]	–	470	6.4	1.36×10^{-2}
7.5	16±1	325±2	4.0±0.2	$(1.23\pm0.06)\times10^{-2}$
8.15[a]	–	120	2.4	2.0×10^{-2}
8.5	1.36±0.05	n.d.[b]	n.d.[b]	n.d.[b]
9.15[a]	–	42	1.1	2.6×10^{-2}

[a] Ref [30]
[b] n.d.=not determined

$0.4)\times10^2$ M^{-1} s^{-1}. With increasing pH the second-order rate constant decreased continuously to k_3=1.36± 0.05 M^{-1} s^{-1} at pH 8.5. The large error of the value at pH 6.1 is due to the instability of the MbFe^{IV}=O solution under acidic conditions [46, 47, 48]. This instability did not cause any problems for the determination of the rate constant of the reaction with NO˙ because this latter reaction proceeds at a significantly faster rate. In addition, at low pH and in the presence of a large excess of nitrite a second reaction was observed in the course of the stopped-flow measurements. The presence of this reaction, which corresponds to the subsequent binding of nitrite to metMb, also interfered with the exact determination of the rate constant of the reaction between nitrite and MbFe^{IV}=O.

In order to be able to confirm that the second reaction observed was indeed that between nitrite and metMb, we determined its rate constant in an independent experiment under the same experimental conditions. The kinetics were studied by stopped-flow spectroscopy with nitrite in at least 10-fold excess by following the absorbance changes at 410 or 575 nm. The plot of the observed pseudo-first-order rate constant versus nitrite concentration showed a saturation behavior at nitrite concentrations above 100 mM (data not shown). However, a second-order rate constant could be obtained from the linear part of the plots in the range 5–40 mM. As shown from the data summarized in Table 3, the binding rate of nitrite to metMb decreases with increasing pH and is always faster than the corresponding rate of reaction of nitrite with MbFe^{IV}=O. At pH 6.7 and 20 °C the binding rate is k_4=(8.1±0.2)×10^2 M^{-1} s^{-1}, a value comparable to that reported in the literature (4.7×10^2 M^{-1} s^{-1} at pH 7.0 and 21–23 °C [30]). The dissociation rate, obtained from the intercept of the linear plot, is k_{-4}=9.8±0.3 s^{-1} at pH 6.7, and decreases with increasing pH (Table 3). This value is also in agreement with that reported in the literature (6.4 s^{-1} at pH 7.0 and 21–23 °C [30]).

As the reaction of MbFe^{IV}=O with nitrite is very slow and the MbFe^{IV}=O solutions are not indefinitely stable [46, 47, 48], it proved impossible to determine the yield of the nitrite-mediated reduction of MbFe^{IV}=O. Indeed, the reaction of one equivalent of nitrite with MbFe^{IV}=O is slower than the autoreduction of MbFe^{IV}=O to metMb.

Table 4 Amount of nitrite formed from the reaction of MbFe^{IV}=O with one equivalent of NO˙. Comparison between the amount of nitrate found after the reaction and that present in the NO˙ solution

1 pH	2 [MbFe^{IV}=O] (µM)	3 [NO$_2^-$][a] (µM)	4 Measured [NO$_3^-$] in NO˙ soln.[b] (µM)	5 [NO$_3^-$] in NO˙ soln.[c] (µM)
7.0	47.3	46.6	4.3	4.3
7.0	47.3	47.6	4.3	3.0
9.5	37.2	38.3	4.1	0.2
9.5	37.2	39.6	4.1	0.4

[a] Concentration of nitrite ions generated from the reaction of MbFe^{IV}=O with NO˙, calculated from the concentration of nitrite ions found in the reaction solution minus the concentration of nitrite already present in the added NO˙ solution
[b] Nitrate contamination of the NO˙ solutions determined separately as described in Materials and methods
[c] Concentration of nitrate ions generated from the reaction of MbFe^{IV}=O with NO˙, calculated from the concentration of nitrate ions found in the reaction solution minus the concentration of nitrate already present in the added NO˙ solution (column 4)

Analysis of the nitrogen-containing products

The determination of the amount of nitrite and nitrate ions formed from the reaction of MbFe^{IV}=O with one equivalent of NO˙ at pH 7.0 and 9.5 was carried out by anion chromatography with conductivity detection. As shown in Table 4 (columns 2 and 3), nitrite was always formed quantitatively from the NO˙-mediated reduction of MbFe^{IV}=O. The concentration of nitrate remained approximately unchanged during the course of the reaction (columns 4 and 5 in Table 4).

As the nitrite-mediated reduction of MbFe^{IV}=O is very slow, the identification of the nature of the nitrogen-containing products had to be carried out by mixing an excess of nitrite with MbFe^{IV}=O. At pH 7.0, we found that one equivalent of nitrite, relative to the amount of MbFe^{IV}=O, was transformed to half an equivalent of nitrite plus half an equivalent of nitrate (columns 6 and 7 in Table 5).

Table 5 Amount of nitrite and nitrate formed from the reaction of MbFe^{IV}=O with an excess of nitrite

1 pH	2 [MbFe^{IV}=O] (µM)	3 Added [NO$_2^-$] (µM)	4 Ex. [NO$_2^-$][a] (µM)	5 Found [NO$_2^-$][b] (µM)	6 [NO$_2^-$][c] (µM)	7 [NO$_3^-$][d] (µM)
7.0	25.7	216.3 (25.7+190.6)	190.6	203.9 (13.3+190.6)	13.3	14.1
7.0	43.2	248.9 (43.2+205.7)	205.7	226.4 (20.7+205.7)	20.7	22.2

[a] Concentration of nitrite added in excess, by considering that only one equivalent reacts with MbFe^{IV}=O

[b] Total concentration of nitrite ions found in the protein solution after reaction

[c] Concentration of nitrite ions generated from the reaction of MbFe^{IV}=O with one equivalent of nitrite, calculated from the total concentration of nitrite ions found in the protein solution after reaction (column 5) minus the concentration of the excess nitrite ions added (column 4)

[d] Concentration of nitrate ions in the protein solution after reaction with nitrite

Nitration of tyrosine by the MbFe^{IV}=O/nitrite reaction system

Nitrogen dioxide may be generated from the reaction of MbFe^{IV}=O with nitrite. As it is known that NO$_2^·$ is a potent nitrating agent [17, 24], it was of interest to find out whether 3-nitrotyrosine (NO$_2$-Tyr) is generated in the course of the nitrite-mediated reduction of MbFe^{IV}=O. We thus analyzed the amino acids obtained after complete acid hydrolysis of the reacted protein by HPLC, but no nitrotyrosine was detected. In contrast, when free tyrosine was added to nitrite prior to its reaction with MbFe^{IV}=O, less than 1% nitrotyrosine, relative to the protein, was generated. As shown in Table 6 (entries 1–3), the yield of nitrotyrosine slightly increased with increasing nitrite concentrations.

Finally, we were interested to find out whether NO$_2$-Tyr was generated when ·MbFe^{IV}=O was mixed with nitrite in the presence of Tyr. As summarized in Table 6 (entries 4–7), when H$_2$O$_2$ was added to a mixture of nitrite, Tyr, and metMb, significantly larger amounts of NO$_2$-Tyr were formed. The yield of NO$_2$-Tyr increased with increasing nitrite concentrations.

Table 6 Entries 1–3: yield of NO$_2$-Tyr (% relative to metMb) from the reaction of MbFe^{IV}=O [generated by allowing to react a solution of metMb (250 µM) with 1 equiv of H$_2$O$_2$ (250 µM) for 6 min] with a solution containing 4 equiv of Tyr (1 mM) and variable amounts of nitrite. Entries 4–7: yield of NO$_2$-Tyr (% relative to metMb) from the reaction of a solution of metMb (250 µM), 4 equiv of Tyr (1 mM), and variable amounts of nitrite with a solution containing 1 equiv of H$_2$O$_2$ (250 µM)

Entry	[NO$_2^-$] (mM)	Yield NO$_2$-Tyr (% relative to metMb)
1	1.0	0.28±0.02
2	2.5	0.31±0.01
3	7.5	0.36±0.01
4	1.0	3.1±0.1
5	2.5	5.1±0.2
6	5.0	7.8±0.1
7	7.5	12.9±0.4

Discussion

Nitrogen monoxide (NO$^·$) is currently a species of extreme biological interest because of the variety of physiological and pathophysiological functions which have been found to be associated with this inorganic messenger molecule [49, 50, 51]. The cytotoxic effects of NO$^·$ originate mainly from its reaction with superoxide to generate the powerful oxidizing and nitrating agent peroxynitrite. In contrast, NO$^·$ has also been reported to display antioxidant effects [3, 15, 17, 18, 19], either by scavenging free radicals to generate less reactive nonradical species [17, 52] or by inactivating catalytically active high-valent hemoprotein intermediates [15, 18].

In a recent paper, Gorbunov et al. [16] reported that the oxoiron(IV) myoglobin species MbFe^{IV}=O and ·MbFe^{IV}=O react with NO$^·$ to generate metMb. In addition, they showed by ESR and electrospray MS analysis that, in the course of the reaction, no covalent adducts were generated between NO$^·$ and the globin or the heme [53]. The reaction of NO$^·$ with high-valence myoglobin species has thus been proposed to represent a potential antioxidant role for NO$^·$. However, the determination of the rate constant is essential in order to evaluate the biological relevance of this reaction. In the present work, we carried out detailed kinetic and mechanistic analyses of the NO$^·$-mediated reduction of MbFe^{IV}=O.

The reaction between MbFe^{IV}=O and NO$^·$ is shown to proceed via the rapid formation of an intermediate, which then decays to metMb and nitrite. At pH 7.5 and 20 °C the second-order rate constant for the formation of this intermediate is $(17.9±0.5)×10^6$ M^{-1} s^{-1} and that for its decay is 3.36±0.05 s^{-1}. The spectrum of the intermediate species displays very characteristic absorption maxima at 631 and 504 nm. A comparison with the spectra of other metMb derivatives with anionic ligands such as the nitro- and nitrato-metMb complexes supports the assignment of this species as a high-spin iron(III) complex (Table 2). The position and the intensity of the Soret band are also comparable with the listed derivatives. Because of the radical-like character of the oxo ligand in MbFe^{IV}=O [54, 55,

56, 57], it is reasonable to assume that the first step of the reaction is a fast radical recombination (Scheme 1). The observed intermediate may thus be assigned as the nitrito complex MbFe^{III}ONO. However, the UV-visible spectra of the nitro- (MbFe^{III}NO$_2$) and the nitrito- (MbFe^{III}ONO) metMb complexes are almost identical. This observation may suggest that in a second, very rapid step, MbFe^{III}ONO rearranges to MbFe^{III}NO$_2$. In this case, the observed intermediate would be MbFe^{III}NO$_2$, from which nitrite dissociates in the last step of the reaction.

Nevertheless, several observations can be used to argue against this second possibility. We have recently shown that the spectra of MbFe^{III}NO$_2$, MbFe^{III}ONO$_2$, and MbFe^{III}OONO are also very similar [58]. These three complexes can clearly be distinguished from each other because the rates of dissociation of nitrite and nitrate, respectively, are significantly different [58]. Thus, these results imply that when an anionic ligand is coordinated to metMb, the spectrum is not strongly influenced by the type of atom directly bound to the high-spin iron(III). Unfortunately, as shown in Tables 1 and 3, the rates of dissociation of nitrite from MbFe^{III}ONO (k_2) and from MbFe^{III}NO$_2$ (k_{-4}) are very similar and cannot be used to distinguish between the two complexes. This result was unexpected, as it is known that nitrite preferentially binds via the nitrogen atom to iron. Indeed, no nitrito-iron complexes are known, whereas several nitro-iron(III) complexes, and in particular nitro-iron(III) porphyrin complexes, have been synthesized and structurally characterized [59, 60, 61, 62, 63, 64]. However, the similarity between the two dissociation rates k_2 and k_{-4} might also be a coincidence. The dissociation rate from MbFe^{III}ONO (k_2) has been determined directly with very good accuracy. In contrast, the values for the dissociation rate from MbFe^{III}NO$_2$ (k_{-4}) have been determined indirectly, either from the intercept of the linear plot of the observed pseudo-first-order rate constant versus nitrite concentration (Table 3) or from the product of the equilibrium constant (K_4) and the association constants [30]. These values may thus be associated with large errors.

The observation that the values of the dissociation constants increase with decreasing pH implies that a protonated form of the enzyme facilitates nitrite dissociation. The protonated form of nitrite, HNO$_2$, cannot play a role in this reaction. Indeed, the pK_a value for nitrous acid is 3.3 and HNO$_2$ is thus present only in trace amounts in the pH range studied. With the assumption that the pH dependence originates from a single ionizable residue of the protein, the following relationship between k_2 and the proton concentration can be derived:

$$k_2 = (k'_2 \times [H^+])/(K_a + [H^+]) \tag{1}$$

where k'_2 represents the pH-independent first-order dissociation constant and K_a the dissociation constant of the protonable 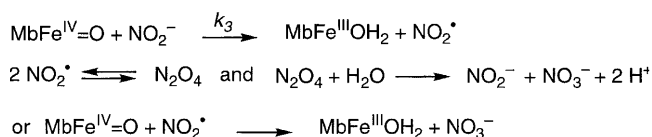residue. Despite the fact that the reaction was studied at only few pH values and thus large errors are associated with the results, the experimental data could be fitted to Eq. 1. The best fit gave a value of pK_a=6.5±0.5 and k'_2=21±5 s^{-1}. These results suggest the involvement of a histidine residue, very likely the distal histidine, which has been shown to be protonated at pH values lower than 6 [65]. In the protonated form this histidine swings out of the heme pocket toward the solvent, with consequent opening of the active site [65] and possible acceleration of the dissociation rate. Interestingly, the rate constants measured for the rate of decay of MbFe^{III}OONO to metMb and nitrate are significantly larger but show the same pH dependence as those obtained for the decay of MbFe^{III}ONO to metMb and nitrite [58].

The rate constant for the reaction of NO$^{\cdot}$ with MbFe^{IV}=O is one order of magnitude larger than that with the corresponding HRP-Compound II (7.4–13×10^5 M^{-1} s^{-1} at pH 7.4 and 20 °C [66]) and three orders of magnitude larger than that with MPO-Fe^{IV}=O (8×10^3 M^{-1} s^{-1} at pH 7.0 and 25 °C [67]). This difference might arise from the negatively charged character of the proximal histidine. The partly deprotonated histidine is likely to stabilize the higher valence form (MbFe^{IV}=O) relative to the radical form (MbFe^{III}-O$^{\cdot}$) and thus slow down the radical recombination (Scheme 1). No intermediate has been reported to be generated in the reaction of NO$^{\cdot}$ with HRP- as well as with MPO-Compound II. This result suggests that dissociation of nitrite from Fe^{III} is much faster for HRP and MPO than for Mb. This difference is not unexpected as it is conceivable that nitrite dissociates faster from the negatively charged MPO- or HRP-[(His$^-$)Fe^{III}NO$_2$] than from the neutral Mb-[(His)Fe^{III}NO$_2$].

Nitrite is one of the major end products of NO$^{\cdot}$ metabolism. It has been shown to be oxidized by peroxidases such as HRP, MPO, and LPO in the presence of hydrogen peroxide, most likely to generate nitrogen dioxide, which can nitrate tyrosine residues free or incorporated into proteins [22, 25]. The rate constants for the reaction of nitrite with MPO-, LPO-, and HRP-Compound II have recently been reported to vary significantly between the three proteins and to be (5.5±0.1)×10^2 M^{-1} s^{-1} (at pH 7.0 and 15 °C [68]), (3.5±0.1)×10^4 M^{-1} s^{-1} and 13.3±0.1 M^{-1} s^{-1}, respectively (at pH 7.0 and room temperature [69]). In the present work we have measured by stopped-flow spectroscopy the rate constant of the reaction between MbFe^{IV}=O and nitrite. The second-order rate constant at pH 7.5 and 20 °C is 16±1 M^{-1} s^{-1}, which is of the same order of magnitude as that for the reaction between nitrite and HRP-Compound II [69], but 1–3 orders of magnitude slower than the corresponding reactions with MPO- and LPO-Compounds II [68, 69]. The pH dependence in the range 6.1–8.5 shows that, as was reported for the reaction of nitrite with MPO-Compound II [68], the rate of reaction between MbFe^{IV}=O and nitrite decreases with increasing pH (Table 3).
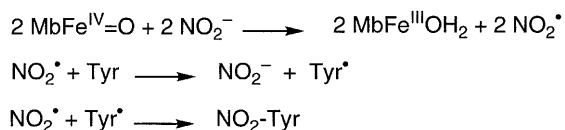
The same trend has been found for the rate of reaction of $MbFe^{IV}=O$ with NADH [70] and that of autoreduction of $MbFe^{IV}=O$ [46]. Also for the reaction of $MbFe^{IV}=O$ with nitrite it can be assumed that the pH dependence originates from a single ionizable residue and thus the experimental data can be fitted to Eq. 1. The best fit gave a value of $pK_a=6.0\pm0.5$ and $k_3'=(52\pm9)\times10$ M^{-1} s^{-1}. Again, the large errors of these numbers are due to the small number of pH values studied. The value obtained for the pK_a of the protonable residue reveals that when the distal histidine is protonated and, thus, turned out toward the solvent, nitrite can diffuse more rapidly into the active site. Alternatively, it has been shown that $MbFe^{IV}=O$, in order to be able to oxidize substrates efficiently, requires the conversion to an activated form in a pH-dependent process [31]. The pK_a of $MbFe^{IV}=O$ has been estimated to be in the region of 6 [71]. Thus, protonation of the ferryl might also be an explanation for the observed increase in the rate of reaction at lower pH values.

Analysis of the nitrogen-containing products of the reaction between $MbFe^{IV}=O$ and nitrite reveals that, as has previously been suggested for the corresponding reactions with peroxidases Compound II [17, 22, 24], nitrogen dioxide may be generated in the first step (Scheme 2). In the absence of added substrates, nitrogen dioxide rapidly dimerizes to N_2O_4, which then hydrolyzes to nitrite and nitrate. Alternatively, nitrate could be generated from the fast reaction between $MbFe^{IV}=O$ and $NO_2^{\cdot}$ [58].
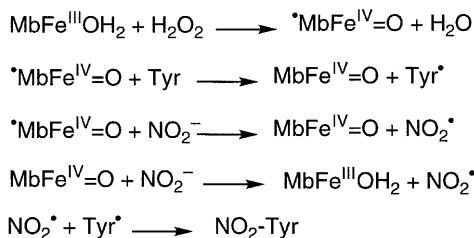
$$MbFe^{IV}=O + NO_2^- \xrightarrow{k_3} MbFe^{III}OH_2 + NO_2^{\bullet}$$

$$2\,NO_2^{\bullet} \rightleftharpoons N_2O_4 \quad and \quad N_2O_4 + H_2O \longrightarrow NO_2^- + NO_3^- + 2\,H^+$$

$$or \quad MbFe^{IV}=O + NO_2^{\bullet} \longrightarrow MbFe^{III}OH_2 + NO_3^-$$

Scheme 2

In the presence of added tyrosine, $NO_2^{\cdot}$ leads to the production of very small amounts of 3-nitrotyrosine (NO_2-Tyr) (Table 6, entries 1–3), which are likely to be formed from the fast recombination of $NO_2^{\cdot}$ with a tyrosyl radical (Tyr$^{\cdot}$) [23]. Two sources are available to generate a tyrosyl radical from tyrosine. $NO_2^{\cdot}$ can react with Tyr to yield Tyr$^{\cdot}$ at a rate of about 10^5 M^{-1} s^{-1} [23] or, alternatively, $MbFe^{IV}=O$ can oxidize Tyr. As the latter reaction proceeds at a rate of about 40 M^{-1} s^{-1} (data not shown), this pathway is probably less relevant. The reaction is thus likely to proceed as shown in Scheme 3. The very low yield of

$$2\,MbFe^{IV}=O + 2\,NO_2^- \longrightarrow 2\,MbFe^{III}OH_2 + 2\,NO_2^{\bullet}$$

$$NO_2^{\bullet} + Tyr \longrightarrow NO_2^- + Tyr^{\bullet}$$

$$NO_2^{\bullet} + Tyr^{\bullet} \longrightarrow NO_2\text{-Tyr}$$

Scheme 3

$$MbFe^{III}OH_2 + H_2O_2 \longrightarrow {}^{\bullet}MbFe^{IV}=O + H_2O$$

$${}^{\bullet}MbFe^{IV}=O + Tyr \longrightarrow MbFe^{IV}=O + Tyr^{\bullet}$$

$${}^{\bullet}MbFe^{IV}=O + NO_2^- \longrightarrow MbFe^{IV}=O + NO_2^{\bullet}$$

$$MbFe^{IV}=O + NO_2^- \longrightarrow MbFe^{III}OH_2 + NO_2^{\bullet}$$

$$NO_2^{\bullet} + Tyr^{\bullet} \longrightarrow NO_2\text{-Tyr}$$

Scheme 4

NO_2-Tyr is probably due to the concurrent fast reaction of $NO_2^{\cdot}$ with $MbFe^{IV}=O$ (Scheme 2) [58].

Significantly larger amounts of NO_2-Tyr were obtained when nitrite was reacted in situ with $^{\cdot}MbFe^{IV}=O$ in the presence of added free tyrosine (Table 6, entries 4–7). These results indicate that, in order to generate higher yields of NO_2-Tyr, a further source of tyrosyl radicals must be present in the system. Indeed, Tyr$^{\cdot}$ may be first generated from the reaction of Tyr with $^{\cdot}MbFe^{IV}=O$ and then rapidly recombine with $NO_2^{\cdot}$ (Scheme 4). At higher nitrite concentrations, larger amounts of $NO_2^{\cdot}$ are formed, possibly also from the reaction of nitrite with $^{\cdot}MbFe^{IV}=O$, and trap Tyr$^{\cdot}$ more efficiently, resulting in larger yields of NO_2-Tyr. This in situ reaction should represent a better model for the physiological conditions, as it is more likely that all the reagents are present contemporaneously. Thus, our data imply that the reaction of H_2O_2 with metMb in the presence of nitrite may represent an alternative route, in addition to peroxynitrite-mediated nitration [26, 27, 28], to generate nitrotyrosine in vivo.

Conclusions

In the present work we have determined the rate constant for the reaction between $MbFe^{IV}=O$ and $NO^{\cdot}$ to be $(17.9\pm0.5)\times10^6$ M^{-1} s^{-1} at pH 7.5 and 20 °C. This reaction proceeds at a rate comparable to that for the reaction between $MbFeO_2$ and $NO^{\cdot}$ $\{(43.6\pm0.5)\times10^6$ M^{-1} s^{-1} at pH 7.5 and 20 °C [58]$\}$. Thus, it may represent a valid alternative reaction between myoglobin and $NO^{\cdot}$. The high-valence form of Mb has been proposed to be at least in part responsible for oxidative lesions found on ischemic/reperfused tissues [6]. Other one-electron reductants present in vivo such as ascorbate react with $MbFe^{IV}=O$ at a significantly lower rate (2.7 ± 0.8 10^6 M^{-1} s^{-1} at pH 7.0 and 25 °C) [13]. Therefore, as the products generated from the reaction of $MbFe^{IV}=O$ with $NO^{\cdot}$ are not strong oxidizing species, this reaction might represent a pathway for detoxification of $MbFe^{IV}=O$ in vivo.

In contrast, the reaction between nitrite and $MbFe^{IV}=O$ proceeds at a significantly lower rate (16 ± 1 M^{-1} s^{-1} at pH 7.5 and 20 °C) and generates the nitrating agent nitrogen dioxide. Our results suggest that this reaction may play a role only in the absence

of peroxynitrite, which also reacts significantly faster with MbFe^{IV}=O {$(2.2\pm0.1)\times10^4$ M^{-1} s^{-1} at pH 7.3 and 20 °C [72]}, or when NO$^{.}$ has been completely converted to nitrite. However, we have also shown that, in the presence of nitrite and added free tyrosine, the reaction of metMb with H$_2$O$_2$ can yield significant amounts of NO$_2$-Tyr. Under pathophysiological conditions in which the nitrite level can be elevated, this reaction may thus contribute to nitration of tyrosine residues either free or incorporated into proteins. The results reported are important for a better understanding of the interaction of NO$^{.}$ with hemoproteins with oxidase activity under inflammatory or ischemic conditions, when generation of NO$^{.}$, nitrite, and H$_2$O$_2$ is elevated.

References

1. Gunther MR, Sampath V, Caughey WS (1999) Free Radical Biol Med 26:1388–1395
2. Turner JJO, Rice-Evans CA, Davies MJ, Newman ES (1990) Biochem Soc Trans 18:1056–1059
3. Grisham MB, Granger DN, Lefer DJ (1998) Free Radical Biol Med 25:404–433
4. Grisham MB, Everse J (1991) In: Everse J, Everse KE, Grisham MB (eds) Peroxidases in chemistry and biology. CRC Press, Boston, pp 335–344
5. Chance B, Sies H, Boveris A (1979) Physiol Rev 59:527–605
6. Galaris D, Eddy L, Arduini A, Cadenas E, Hochstein P (1989) Biochem Biophys Res Commun 160:1162–1168
7. Giulivi C, Cadenas E (1994) Methods Enzymol 233:189–202
8. Harel S, Kanner J (1988) Free Radical Res Commun 5:21–33
9. Berzofsky JA, Peisach J, Blumberg WE (1971) J Biol Chem 246:3367–3377
10. Arduini A, Eddy L, Hochstein P (1990) Free Radical Biol Med 9:511–513
11. Galaris D, Sevanian A, Cadenas E, Hochstein P (1990) Arch Biochem Biophys 281:163–169
12. Newman ESR, Rice-Evans CA, Davies MJ (1991) Biochem Biophys Res Commun 179:1414–1419
13. Kröger-Ohlsen M, Skibsted LH (1997) J Agric Food Chem 45:668–676
14. Dee G, Rice-Evans C, Obeyesekera S, Meraji S, Jacobs M, Bruckdorfer KR (1991) FEBS Lett 294:38–42
15. Wink DA, Hanbauer I, Laval F, Cook JA, Krishna MC, Mitchell JB (1994) In: Chiueh CC, Gilbert DL, Colton CA (eds) Annual review of the New York Academy of Science. New York Academy of Science, New York, pp 265–278
16. Gorbunov NV, Osipov AN, Day BW, Zayas-Rivera B, Kagan VE, Elsayed NM (1995) Biochemistry 34:6689–6699
17. Wink DA, Cook JA, Krishna MC, Hanbauer I, DeGraff W, Gamson J, Mitchell JB (1995) Arch Biochem Biophys 319:402–407
18. Jourd'heuil D, Mills L, Miles AM, Grisham MB (1998) Nitric Oxide Biol Chem 2:37–44
19. Gorbunov NV, Tyurina YY, Salama G, Day BW, Claycamp HG, Argyros G, Elsayed NM, Kagan VE (1998) Biochem Biophys Res Commun 244:647–751
20. Kaur H, Halliwell B (1994) FEBS Lett 350:9–12
21. Torre D, Ferrario G, Speranza F, Orani A, Fiori GP, Zeroli C (1996) J Clin Pathol 49:574–576
22. Klebanoff SJ (1993) Free Radical Biol Med 14:351–360
23. Prütz WA, Mönig H, Butler J, Land EJ (1985) Arch Biochem Biophys 243:125–134
24. Goss SPA, Singh RJ, Hogg N, Kalyanaraman B (1999) Free Radical Res 31:597–606
25. van der Vliet A, Eiserich JP, Halliwell B, Cross CE (1997) J Biol Chem 272:7617–7625
26. Reiter CD, Teng R-J, Beckman JS (2000) J Biol Chem 275:32460–32466
27. Souza JM, Daikhin E, Yudkoff M, Raman CS, Ischiropoulos H (1999) Arch Biochem Biophys 371:169–178
28. Ischiropoulos H (1998) Arch Biochem Biophys 356:1–11
29. Østdal H, Daneshvar B, Skibsted LH (1996) Free Radical Res 24:429–438
30. Antonini E, Brunori M (1971) Hemoglobin and myoglobin in their reactions with ligands. North-Holland, Amsterdam
31. Fenwick CW, English AM, Wishart JF (1997) J Am Chem Soc 119:4758–4764
32. Herold S (1999) Arch Biochem Biophys 372:393–398
33. Giulivi C, Cadenas E (1998) Free Radical Biol Med 24:269–279
34. Gunther MR, Sturgeon BE, Mason RP (2000) Free Radical Biol Med 28:709–719
35. Schmidt HHHW, Kelm M (1996) In: Feelisch M, Stamler JS (eds) Methods in nitric oxide research. Wiley, New York, pp 491–497
36. George P, Irvine DH (1952) Biochem J 52:511–517
37. Tajima G-I, Shikama K (1993) Int J Biochem 25:101–105
38. Herold S (1999) FEBS Lett 443:81–84
39. Sono M, Dawson JH (1982) J Biol Chem 257:5496–5502
40. King NK, Winfield ME (1963) J Biol Chem 238:1520–1528
41. Osawa Y, Korzekwa K (1991) Proc Natl Acad Sci USA 88:7081–7085
42. Gunther MR, Hsi LC, Curtis JF, Gierse JK, Marnett LJ, Eling TE, Mason RP (1997) J Biol Chem 272:17086–17090
43. Goodwin DC, Gunther MR, Hsi LC, Crews BC, Eling TE, Mason RP, Marnett LJ (1998) J Biol Chem 273:8903–8909
44. Sanakis Y, Goussias C, Mason RP, Petrouleas V (1997) Biochemistry 36:1411–1417
45. Szalai VA, Brudvig GW (1996) Biochemistry 35:15080–15087
46. Kröger-Ohlsen MV, Andersen ML, Skibsted LH (1999) Free Radical Res 30:305–314
47. Wazawa T, Matsouka A, Tajima G, Sugawara Y, Nakamura K, Shikama K (1992) Biophys J 63:544–550
48. Alayash AI, Brockner Ryan BA, Eich RF, Olson JS, Cashon RE (1999) J Biol Chem 274:2029–2037
49. Moncada S, Palmer RMJ, Higgs EA (1991) Pharmacol Rev 43:109–142
50. Beckman JS, Koppenol WH (1996) Am J Physiol 271:C1424–C1437
51. Wink DA, Feelisch M, Vadovotz Y, Fukuto J, Grisham MB (1999) In: Gilbert DL, Colton CA (eds) Reactive oxygen species in biological systems: an interdisciplinary approach. Kluwer/Plenum, New York, pp 245–291
52. Rubbo H, Freeman BA (1996) Methods Enzymol 269:385–394
53. Osipov AN, Gorbunov NV, Day BW, Elsayed NM, Kagan VE (1996) Methods Enzymol 268:193–203
54. Filatov M, Harris N, Shaik S (1999) J Chem Soc Perkin Trans 2 399–410
55. Sevin A, Fontecave M (1986) J Am Chem Soc 108:3266–3272
56. Hanson LK, Chang CK, Davis MS, Fajer J (1981) J Am Chem Soc 103:663–670
57. Sawyer DT (1987) Comments Inorg Chem 6:103–121
58. Herold S, Exner M, Nauser T (2001) Biochemistry 40:3385–3395
59. Ellison MK, Schulz CE, Scheidt WR (1999) Inorg Chem 38:100–108
60. Munro OQ, Scheidt WR (1998) Inorg Chem 37:2308–2316

61. Frangione M, Port J, Baldiwala M, Judd A, Galley J, DeVega M, Linna K, Caron L, Anderson E, Goodwin JA (1997) Inorg Chem 36:1904–1911
62. Nasri H, Haller KJ, Wang Y, Huynh BH, Scheidt WR (1992) Inorg Chem 31:3459–3467
63. Nasri H, Wang Y, Huynh BH, Walker FA, Scheidt WR (1991) Inorg Chem 30:1483–1489
64. Nasri H, Goodwin JA, Scheidt WR (1990) Inorg Chem 29:185–191
65. Miller LM, Patel M, Chance MR (1996) J Am Chem Soc 118:4511–4517
66. Glover RE, Koshkin V, Dunford HB, Mason RP (1999) Nitric Oxide Biol Chem 3:439–444
67. Abu-Soud HM, Hazen SL (2000) J Biol Chem 275:37524–37532
68. Burner U, Furtmüller PG, Kettle AJ, Koppenol WH, Obinger C (2000) J Biol Chem 275:20597–20601
69. Gebicka L (1999) Acta Biochim Polon 46:919–927
70. Mikkelsen A, Skibsted LH (1995) Z Lebensm Unters Forsch 200:171–177
71. Foote N, Gadsby PMA, Greenwood C, Thomson AJ (1989) Biochem J 261:515–522
72. Exner M, Herold S (2000) Chem Res Toxicol 13:287–293